Floquet analysis of secondary instability of boundary layers distorted by Klebanoff streaks and Tollmien–Schlichting waves

Yang Liu,[1] Tamer A. Zaki,[2] and Paul A. Durbin[3]
[1]*Department of Mechanical Engineering, Stanford University, Stanford, California 94305, USA*
[2]*Department of Mechanical Engineering, Imperial College London, London SW7 2AZ, United Kingdom*
[3]*Department of Aerospace Engineering, Iowa State University, Ames, Iowa 50011, USA*

(Received 27 September 2007; accepted 2 November 2008; published online 11 December 2008)

Previous studies of the interaction between boundary layer streaks and Tollmien–Schlichting (TS) waves have shown puzzling effects. Streaks were shown to reduce the growth rate of primary TS waves and, thereby, to delay transition; however, they can also promote transition by inducing a secondary instability. The outcome of the interaction depends on the spanwise wavelength and intensity of the streaks as well as on the amplitude of the TS waves. A Floquet analysis of secondary instability is able to explain many of these features. The base state is periodic in two directions: it is an *Ansatz* composed of a saturated TS wave (periodic in x) and steady streaks (periodic in z). Secondary instability analysis is extended to account for the doubly periodic base flow. Growth rate computations show that, indeed, the streak can either enhance or diminish the overall stability of the boundary layer. The stabilizing effect is a reduction in the growth rate of the primary two-dimensional TS wave; the destabilizing effect is a secondary instability. Secondary instability falls into two categories, depending on the spanwise spacing of the streaks. The response of one category to perturbations is dominated by fundamental and subharmonic instability; the response of the other is a detuned instability. © *2008 American Institute of Physics*. [DOI: 10.1063/1.3040302]

I. INTRODUCTION

Transition to turbulence in boundary layers is often classified as either orderly or as bypass. The orderly route refers to the amplification, secondary instability, and breakdown of discrete Tollmien–Schlichting (TS) waves. Instances of boundary layer breakdown which deviated from this description have generally been termed bypass, with the most common bypass scenario being transition due to forcing by free-stream turbulence. In this instance, a fully turbulent boundary layer can be established at subcritical Reynolds numbers, and thus unstable TS waves are entirely absent. Instead, transition is preceded by the formation of high-amplitude, streamwise-elongated disturbances known as Klebanoff distortions or streaks.

Bypass transition is not always free from TS waves. For instance, in adverse pressure gradient the critical Reynolds number for TS waves is sufficiently low that they may coexist and interact with boundary layer streaks. Theory, computer simulation, and physical experiments have raised basic questions on how "streaks" influence the evolution of TS waves, their secondary instability, and finally breakdown into turbulence. Some studies show that, in the presence of small amplitude streaks, the boundary layer is more unstable.[1] Others show that streaks suppress the amplification of primary TS waves,[2–4] yet transition is promoted.[2,4] Our recent direct numerical simulation (DNS) studies[5,6] provide some degree of empirical resolution: streaks do, indeed, reduce the growth rate of primary TS waves and therefore can delay transition. Nevertheless, streaks can also enhance transition by promoting the formation of Λ shaped velocity contours, which precede the appearance of turbulent spots and breakdown of the boundary layer.

How can these apparently conflicting observations be understood? Λ-vortices are familiar from the literature on secondary instability. Herbert[7] provided an explanation via Floquet analysis of an *Ansatz* constructed as a TS wave superimposed on a Blasius profile. He concluded that parametric instability explained the formation of Λ patterns. The Λ patterns that emerge in the presence of streaks are of a different character.[6] They are related to the spanwise wavelength of streaks, which is typically one-tenth that of Herbert's secondary instability. Nevertheless Herbert's Floquet theory suggests a hypothesis for some of the observations of the effect of streaks on TS waves. Our hypothesis is that a competition exists between the reduction in growth rate of primary TS waves[3,1] and a secondary instability. Thus, if the secondary instability is weak, the flow becomes more stable due to the first mechanism; if it is not weak, streaks will promote transition via a secondary instability. In this paper we pursue this hypothesis by an extended Floquet analysis.

Our hypothesis introduces a complication: it implies that both the TS wave amplitude and the streak intensity play roles. We must address a doubly periodic Floquet analysis: the streaks are periodic in z; the TS waves are periodic in x. The analysis follows Herbert[7] in supposing a TS *Ansatz* and Cossu and Brandt[3] in invoking a streak *Ansatz*, but now they must be included simultaneously.

Before proceeding to the analysis, we must discuss the notion of a streak, which can be modeled and generated experimentally in a variety of ways. The widely used terminology presupposes that the particulars of the streak are not critical to the phenomena being investigated. That does, in-

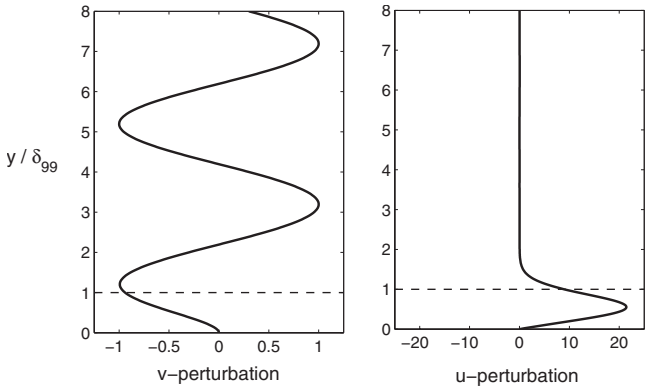

FIG. 1. The linear boundary layer response to a continuous OS mode forcing. At left, the OS continuous mode, and at right the u-perturbation response, obtained by solving the Squire initial value problem.

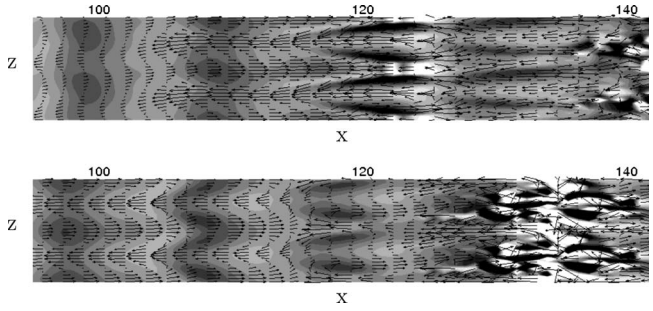

FIG. 2. Plane view showing contours of the instantaneous wall-normal fluctuations and vectors of the in-plane velocity at $y=0.5\delta_{99}$. The Λ pattern is a secondary instability of the primary TS waves in the presence of wide streaks (mode 2: $\beta\delta_*=0.54$, $\lambda_z=11.6\delta_*$).

deed, appear to be the case: various *Ansätze* have been used in numerical studies[3,4,6] with similar results regarding the influence of streaks on the growth rate of primary TS waves. In the laboratory, streaks can not only be artificially excited by rods[8] but also naturally develop in response to forcing by free-stream turbulence.[2,9] In the last case they are called Klebanoff streaks and are quite commonly seen. The term *streak* has its origin in flow visualization. For analytical purposes a less graphical description is warranted. The dominant features are u-component perturbations, which oscillate periodically in the span between positive and negative perturbations of the mean velocity (cf. $u' \propto \cos k_z z$). They are very long in the streamwise direction, having the character of perturbation jets, flowing forward and backward relative to the mean. The dominance of the u component can be explained as the effect of displacement of the mean shear, with the most persistent displacement being highly elongated in the direction of the stream.[10] It is because the key feature is a jetlike perturbation that the same phenomenology has been found with various, *ad hoc*, *Ansätze* to model the streak.

One *Ansatz* for the streaks follows naturally from the boundary layer response to three-dimensional Orr–Sommerfeld (OS) continuous modes. This is a good model for the formation of Klebanoff streaks beneath free-stream turbulence. In linear analysis, the three-dimensional OS mode v appears as a source term in the Squire equation. The Squire response is obtained by solving an initial value problem (Appendix to Zaki and Durbin[11]) and, in the solution, the u velocity is a superposition of Squire modes; it has a y profile quite like those seen in Klebanoff streaks (Fig. 1). The generation of streaks by OS continuous modes was used in DNS studies[6,11,12] and will be adopted for our Floquet analysis.

A. Summary of previous empirical observations

The observation that streaks reduce the amplification of the *primary* TS waves is supported by a number of experimental and numerical investigations. For instance, in the work of Boiko *et al.*,[2] it was noted that streaks induced by free-stream turbulence decrease the growth rate of TS waves generated by a vibrating ribbon. In DNSs by Fasel,[4] it was noted that streaks, induced by volume forcing from the free-stream, have a similar effect on TS waves. These and similar empirical observations, both from experiments and simulations, have been supported by the Floquet analysis of Cosso and Brandt.[13] That analysis showed that the growth rate of the most unstable eigenvalue of the OS equation is reduced when the boundary layer profile is modified by the presence of their model streaks.

Evidence of the exact role of streaks in promoting secondary instability and breakdown of TS waves is more scarce. Experiments that focused on the stabilizing effect of streaks, for example, the work of Fransson *et al.*,[8] did not report the transition mechanism. Others, for instance, the experiments of Boiko *et al.*,[2] reported early transition in the presence of streaks, but did not discuss the effect of the intensity of streaks on the breakdown process.

Recently, we have carried out DNS with the objective of detailing the influence of the streaks on both the growth rate of primary TS waves and their breakdown to turbulence.[6] In the DNS, interaction between discrete and continuous modes was found to depend on the spanwise wave number of the latter. The numerical experiments were for streaks with nondimensional spanwise wave numbers, $0.25<\beta\delta_*<1.5$, based on the displacement thickness. Two broad classes of behavior were seen in the computer experiments and correspond to the influence of a "wide" versus "narrow" streak. The former is epitomized by a streak of spanwise size $\lambda_z=11.6\delta_*$ ($\beta\delta_*=0.54$), which Liu *et al.*[6] referred to as mode 2 because it corresponds to two wavelengths across the span of their computational domain of size $L_z=23\delta_*$. The influence of the narrow streak is epitomized by a continuous mode with spanwise size $\lambda_z=4.6\delta_*$ ($\beta\delta_*=1.35$), which Liu *et al.*[6] referred to as mode 5. (In the study of Liu *et al.*[6] where the DNS was described in detail, the spanwise wave number of the streaks, $\beta=n2\pi/L_z$, was quoted in terms of n, the number of waves that was fitted into the width of the computational domain of size Lz. In this paper, we will always quote both the value of β nondimensionalized by δ_* and the mode number n for the benefit of the readers who wish to compare the current results to those of Liu *et al.*[6])

Figure 2 shows two instants from a flow visualization. It is difficult to see the full pattern of Λ's from a single frame because the Λ-structures at the right are breaking into turbu-

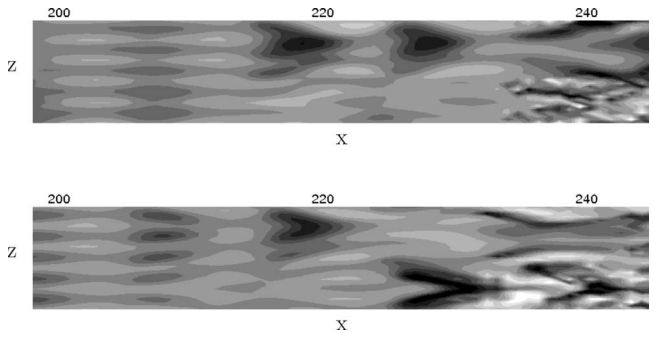

FIG. 3. Instantaneous contours of the streamwise fluctuations showing the secondary instability of TS waves in the presence of narrow streaks (mode 5: $\beta\delta_*=1.35$, $\lambda_z=4.6\delta_*$).

lence and the Λ-structures at the left are still weak, but it becomes evident when a time sequence is visualized at regular intervals. The z spacing between Λ's at a given x location is equal to the wavelength of the continuous mode.

The narrow streaks produced a more irregular pattern, but still containing Λ's. Unlike the wide streak case, the spanwise spacing of the Λ's differed from that of the continuous mode; it appeared to be approximately three times the streak width. Figure 3 contains two snapshots from this case. By contouring the u component, Fig. 3 brings out the streaks; they appear as long contours in the x direction. By contouring v, Fig. 2 brings out the TS waves. They are the bands in the z direction.

Another curious difference between the narrow and wide cases is the influence of the amplitude of the continuous mode on transition location. Klebanoff distortions of large spanwise size cause transition to move upstream with increased streak amplitude. In this case, one can conceive that the spanwise periodic streaks distort the two-dimensional TS wave to create the Λ vortices. This interaction is more effective at higher streak amplitude.

However, this interaction is not inevitable. Indeed, the narrow streak simulations yield interesting results. At low amplitude transition is promoted, but as the amplitude increases transition is *delayed*. If the previously mentioned hypothesis that a competition between suppression of primary TS growth and promotion of secondary instability is correct, then the following explanation can be offered. Low amplitude streaks permit the primary TS waves to grow to sufficient amplitude that they are subjected to secondary instability. However, larger streak amplitude suppresses TS growth, increasing the downstream distance before the TS amplitude is great enough for secondary instability to occur. Transition is delayed thereby.

In this paper, we present a doubly periodic Floquet analysis in order to study the stability of the boundary layer in the presence of two-dimensional TS waves (periodic in x) and steady streaks (periodic in z). The paper is divided into eight sections. In Sec. II, the secondary instability equations are summarized, and the numerical implementation of the solution is described in Sec. III (the validation against published literature is deferred to Appendix). In Secs. IV and V, Floquet analyses are carried out in the presence of either the TS waves or the streaks, alone. Finally, the results from the doubly periodic analysis are presented in Secs. VI and VII, followed by a discussion in Sec. VIII.

II. THEORETICAL FORMULATION

A. Secondary instability

The idea of secondary instabilities is quite simple. Assuming the original base flow is $\mathbf{v}_0$, a modification $\mathbf{v}_1$, which is based on the solution of the primary perturbation equation, is added with an amplitude A to define a new base flow,

$$\mathbf{v}_2 = \mathbf{v}_0 + A\mathbf{v}_1. \tag{1}$$

The modification $\mathbf{v}_1$ can, for instance, be a discrete TS wave, a streak, or a superposition of the two. Linear perturbations to this define a new eigenproblem, whose three-dimensional eigensolutions are the secondary instability waves. One has to be aware of the assumptions or approximations made to derive the eigenvalue problem. First, the base flow $\mathbf{v}_0$ is assumed to be locally parallel; in the present case a Blasius boundary layer profile. Second, the amplitude A is assumed to be constant; for a TS wave *Ansatz* v_1 is periodic in x. This can be justified if the primary waves are saturated. Finally, distortions of the $\mathbf{v}_0$ flow by $\mathbf{v}_1$ are ignored.

Similar to the OS and Squire problems for parallel flow, secondary perturbation equations are derived in the case of the spatially periodic base flow of Eq. (1). Let subscript 3 denote the perturbation. The disturbance equations, linearized about $\mathbf{v}_2$, are

$$\left(\frac{1}{\mathrm{Re}}\nabla^2 - \frac{\partial}{\partial t}\right)\xi_3 - \mathbf{v}_2\cdot\nabla\xi_3 - \mathbf{v}_3\cdot\nabla\xi_2 + (\boldsymbol{\omega}_2\cdot\nabla)u_3 + (\boldsymbol{\omega}_3\cdot\nabla)u_2 = 0, \tag{2}$$

$$\left(\frac{1}{\mathrm{Re}}\nabla^2 - \frac{\partial}{\partial t}\right)\eta_3 - \mathbf{v}_2\cdot\nabla\eta_3 - \mathbf{v}_3\cdot\nabla\eta_2 + (\boldsymbol{\omega}_2\cdot\nabla)v_3 + (\boldsymbol{\omega}_3\cdot\nabla)v_2 = 0, \tag{3}$$

$$\left(\frac{1}{\mathrm{Re}}\nabla^2 - \frac{\partial}{\partial t}\right)\zeta_3 - \mathbf{v}_2\cdot\nabla\zeta_3 - \mathbf{v}_3\cdot\nabla\zeta_2 + (\boldsymbol{\omega}_2\cdot\nabla)w_3 + (\boldsymbol{\omega}_3\cdot\nabla)w_2 = 0, \tag{4}$$

where $\boldsymbol{\omega}\equiv\xi\vec{e}_x+\eta\vec{e}_y+\zeta\vec{e}_z$ is the vorticity vector.

In Secs. II B–II D, the above equations are used to derive the secondary instability problem for a base flow composed of the Blasius profile plus (a) a saturated TS wave which is periodic in x, (b) steady streaks periodic in z, and (c) both the TS wave and streaks. The symbols α and β will be used to refer to the streamwise and spanwise wave numbers of the TS wave and streaks, respectively. The wave numbers of the secondary instability will be denoted k_x and k_z.

B. Secondary instability of saturated TS waves

The secondary instability of TS waves was the first theory to successfully explain the origin of Λ-structures.[7] Let us review this theory as background to our new analysis. It is also a subset of our problem, which provides verification of our computer code.

Upon specifying $\mathbf{v}_1$ as a saturated TS wave, Eq. (1) becomes

$$\mathbf{v}_2(x,y,t) = U_0(y)\vec{e_x} + A[u_{\mathrm{TS}}(x,y,t)\vec{e_x} + v_{TS}(x,y,t)\vec{e_y}], \quad (5)$$

where $U_0(y)$ is the Blasius profile and A is the amplitude of the saturated TS wave. In the *Ansatz*, TS waves are periodic in the streamwise direction and move forward at a constant phase speed. After a change from the laboratory to a Galilean frame,

$$x' = x - c_r t, \quad (6)$$

this is expressed as

$$\mathbf{v}_{\mathrm{TS}}(x,y,t) = \mathbf{v}_{\mathrm{TS}}(x',y), \quad (7)$$

where $\mathbf{v}_{\mathrm{TS}}$ is periodic in x'. Hence, the stability equations are a linear eigensystem with periodic coefficients, which defines a Floquet stability problem.

Substituting the expression (5) for the base flow into the perturbation problem [(2)–(4)], the following equations for normal vorticity and the Laplacian of the normal velocity are derived:

$$\left[\frac{1}{\mathrm{Re}}\nabla^2 - (U_0 - c)\frac{\partial}{\partial x'} - \frac{\partial}{\partial t}\right]\frac{\partial \eta_3}{\partial z} + \zeta_0\frac{\partial^2 v_3}{\partial z^2} + A\left[\left(-\frac{\partial \psi_{\mathrm{TS}}}{\partial y}\frac{\partial}{\partial x'} + \frac{\partial \psi_{\mathrm{TS}}}{\partial x'}\frac{\partial}{\partial y} - \frac{\partial^2 \psi_{\mathrm{TS}}}{\partial x' \partial y}\right)\frac{\partial \eta_3}{\partial z} + \frac{\partial^2 \psi_{\mathrm{TS}}}{\partial x'^2}\left(\frac{\partial^2 v_3}{\partial y^2} + \frac{\partial^2 u_3}{\partial x' \partial y}\right) - \frac{\partial^2 \psi_{\mathrm{TS}}}{\partial y^2}\frac{\partial^2 v_3}{\partial z^2}\right] = 0 \quad (8)$$

and

$$\left[\frac{1}{\mathrm{Re}}\nabla^2 - (U_0 - c)\frac{\partial}{\partial x'} - \frac{\partial}{\partial t}\right]\nabla^2 v_3 - \frac{d\zeta_0}{dy}\frac{\partial v_3}{\partial x'} + A\left[\left(-\frac{\partial \psi_{\mathrm{TS}}}{\partial y}\frac{\partial}{\partial x'} + \frac{\partial \psi_{\mathrm{TS}}}{\partial x'}\frac{\partial}{\partial y}\right)\nabla^2 v_3 + \frac{\partial^2 \psi_{\mathrm{TS}}}{\partial x'^2}\left(\frac{\partial \zeta_3}{\partial y} + \frac{\partial \eta_3}{\partial z}\right) - \frac{\partial^2 \psi_{\mathrm{TS}}}{\partial x' \partial y}\left(\frac{\partial \zeta_3}{\partial x'} + \frac{\partial \xi_3}{\partial z}\right) - \frac{\partial \zeta_{\mathrm{TS}}}{\partial x'}\left(2\frac{\partial u_3}{\partial x'} + \frac{\partial v_3}{\partial y}\right) - \frac{\partial \zeta_{\mathrm{TS}}}{\partial y}\frac{\partial v_3}{\partial x'} - \left(u_3\frac{\partial}{\partial x'} + v_3\frac{\partial}{\partial y}\right)\frac{\partial \zeta_{\mathrm{TS}}}{\partial x'}\right] = 0, \quad (9)$$

where ψ_{TS} is the TS wave stream function and $\zeta_{\mathrm{TS}} = -\nabla^2\psi_{\mathrm{TS}}$. A modal representation of the form

$$\mathbf{v}_3(x',y,z,t) = e^{\sigma t}e^{ik_z z}\mathbf{V}(x',y) \quad (10)$$

is invoked, where σ is the complex growth rate and k_z is a real spanwise wave number of the secondary instability. The Floquet theory of differential equations with periodic coefficients indicates that solutions take the general form

$$\mathbf{V}(x',y) = e^{\kappa x'}\tilde{\mathbf{V}}(x',y), \quad (11)$$

where $\tilde{\mathbf{V}}$ periodic in x' with the TS wavelength,

$$\tilde{\mathbf{V}}(x',y) = \tilde{\mathbf{V}}(x' + \lambda_{\mathrm{TS}},y). \quad (12)$$

Hence, $\tilde{\mathbf{V}}(x',y)$ can be expanded in a Fourier series, and $\mathbf{v}_3$ becomes

$$\mathbf{v}_3 = e^{\sigma t}e^{ik_z z}e^{\kappa x'}\sum_{m=-\infty}^{\infty}\hat{\mathbf{v}}_m(y)e^{im\alpha x'}, \quad (13)$$

where α is the TS wave number, $\alpha = 2\pi/\lambda_{\mathrm{TS}}$.

Both σ and κ can be complex; however, only two of the four unknowns, σ_r σ_i κ_r, and κ_i, can be determined by Eqs. (8) and (9). We consider the temporal eigenvalue problem, $\kappa_r = 0$, and κ_i specified. Combining the $e^{\kappa x'}$ and $e^{im\alpha x'}$ terms reveals that κ and $\kappa \pm in\alpha$ lead to identical solutions. Hence, without loss of generality, $-\alpha/2 < \kappa_i \leq \alpha/2$. The choice of κ_i provides a classification of secondary modes: when $\kappa_i = 0$,

$$\mathbf{v}_3^f = e^{\sigma t}e^{i\beta z}\sum_{m=-\infty}^{\infty}\hat{\mathbf{v}}_m(y)e^{im\alpha x'} \quad (14)$$

are called *fundamental* modes; when $\kappa_i = \alpha/2$,

$$\mathbf{v}_3^s = e^{\sigma t}e^{i\beta z}\sum_{m=-\infty}^{\infty}\hat{\mathbf{v}}_m(y)e^{i(m+1/2)\alpha x'} \quad (15)$$

are called *subharmonic* modes. When κ_i takes other values, of the form $\epsilon\alpha/2$

$$\mathbf{v}_3^d = e^{\sigma t}e^{i\beta z}\sum_{m=-\infty}^{\infty}\hat{\mathbf{v}}_m(y)e^{i(m+\epsilon/2)\alpha x'} \quad (16)$$

are called *detuned* modes, where $0 < |\epsilon| < 1$. Herbert[7] noted that the fundamental modes are associated with primary resonance which is related to the *K*-type Λ-structures; subharmonic modes originate from principal parametric resonance which is related to the *H*-type Λ-structures, and also to triad interactions in *C*-type instability.[14] Detuned modes are produced by a combined resonance.

C. Instability modes in streaky boundary layers

The influence of Klebanoff streaks on boundary layer stability is a second subset of our new Floquet analysis. Cossu and Brandt[13] presented an analysis of TS-type instabilities under the influence of steady streaks.

The base-flow *Ansatz* $\mathbf{v}_2$ is now

$$\mathbf{v}_2(y,z,t) = U_0(y)\vec{e_x} + Bu_K(y,z)\vec{e_x}, \quad (17)$$

where u_K is the streak. Since the $u_K \gg v_K$ and $u_K \gg w_K$, the other two components are omitted from streak models. The most significant difference between Eqs. (17) and (5) is that $\mathbf{v}_2$ is dependent on (y,z) in the latter equation and on (x,y) in the former. Carrying out a similar procedure to Sec. II B, the following two governing equations can be derived:

$$\left(\frac{1}{\mathrm{Re}}\nabla^2 - U_0\frac{\partial}{\partial x} - \frac{\partial}{\partial t}\right)\eta_3 + \zeta_0\frac{\partial v_3}{\partial z} - B\left(u_K\frac{\partial \eta_3}{\partial x} + v_3\frac{\partial^2 u_K}{\partial y\,\partial z} + w_3\frac{\partial^2 u_K}{\partial z^2} + \frac{\partial u_K}{\partial y}\frac{\partial v_3}{\partial z} - \frac{\partial u_K}{\partial z}\frac{\partial v_3}{\partial y}\right) = 0, \tag{18}$$

$$\left(\frac{1}{\mathrm{Re}}\nabla^2 - U_0\frac{\partial}{\partial x} - \frac{\partial}{\partial t}\right)\nabla^2 v_3 - \frac{\partial v_3}{\partial x}\frac{\partial \zeta_0}{\partial y} - B\left(u_K\frac{\partial \nabla^2 v_3}{\partial x} - \frac{\partial^2 u_K}{\partial y^2}\frac{\partial v_3}{\partial x} + \frac{\partial^2 u_K}{\partial z^2}\frac{\partial v_3}{\partial x} + 2\frac{\partial u_K}{\partial z}\frac{\partial^2 v_3}{\partial x\,\partial z} - 2\frac{\partial u_K}{\partial z}\frac{\partial^2 w_3}{\partial x\,\partial y} - 2\frac{\partial^2 u_K}{\partial y\,\partial z}\frac{\partial w_3}{\partial x}\right) = 0. \tag{19}$$

Unlike Eqs. (8) and (9) for the secondary instability of two-dimensional TS waves, in the above w_3 cannot be eliminated and, therefore, the continuity equation must also be solved.

The Floquet expansion for this problem is given by

$$\mathbf{v}_3 = e^{\sigma t}e^{ik_x x}\sum_{m=-\infty}^{\infty}\hat{\mathbf{v}}_m(y)e^{i(m+\gamma/2)\beta z}, \tag{20}$$

where $0<|\gamma|\leq 1$ determines the classification of modes. Furthermore, if the base flow is symmetric in the spanwise direction, $u_K(y,z)$ can expressed as $u_K(y)\cos(\beta z)$. Then, perturbations (20) can be divided into separate groups according to their odd or even symmetries.

D. Secondary instability in the presence of TS waves and streaks

When Klebanoff streaks and TS waves are both present and reach large amplitude, secondary instabilities will depend on both. Assuming the modification of the base flow to be a superposition of steady boundary layer streaks and TS waves, the new base-flow *Ansatz* is

$$\mathbf{v}_2(y,z,t) = U_0(y)\vec{e_x} + A[u_{\mathrm{TS}}(x',y)\vec{e_x} + v_{\mathrm{TS}}(x',y)\vec{e_y}] + Bu_K(y,z)\vec{e_x}. \tag{21}$$

The governing equations for the three-dimensional disturbances can be stated as

$$\frac{1}{\mathrm{Re}}\nabla^2\eta_3 - (U_0-c)\frac{\partial \eta_3}{\partial x'} - U_0'\frac{\partial v_3}{\partial z} - A\left[\frac{\partial \psi_{\mathrm{TS}}}{\partial y}\frac{\partial \eta_3}{\partial x'} - \frac{\partial \psi_{\mathrm{TS}}}{\partial x'}\frac{\partial \eta_3}{\partial y} + \frac{\partial \psi_{\mathrm{TS}}}{\partial x'\,\partial y}\eta_3 + \frac{\partial^2 \psi_{\mathrm{TS}}}{\partial x'^2}\xi_3 + \nabla^2\psi_{\mathrm{TS}}\frac{\partial v_3}{\partial z}\right] - B\left[u_K\frac{\partial \eta_3}{\partial x'} + \frac{\partial^2 u_K}{\partial y\,\partial z}v_3 + \frac{\partial^2 u_K}{\partial z^2}w_3 + \frac{\partial u_K}{\partial y}\frac{\partial v_3}{\partial z} - \frac{\partial u_K}{\partial z}\frac{\partial v_3}{\partial y}\right] = \frac{\partial \eta_3}{\partial t}, \tag{22}$$

$$\frac{1}{\mathrm{Re}}\nabla^2(\nabla^2 v_3) - (U_0-c)\frac{\partial \nabla^2 v_3}{\partial x'} + U_0''\frac{\partial v_3}{\partial x'} - A\left[\frac{\partial \psi_{\mathrm{TS}}}{\partial y}\frac{\partial \nabla^2 v_3}{\partial x'} - \frac{\partial \psi_{\mathrm{TS}}}{\partial x'}\frac{\partial \nabla^2 v_3}{\partial y} - \frac{\partial^2 \psi_{\mathrm{TS}}}{\partial x'^2}\left(\frac{\partial \zeta_3}{\partial y} + \frac{\partial \eta_3}{\partial z}\right) + \frac{\partial^2 \psi_{\mathrm{TS}}}{\partial x'\,\partial y}\left(\frac{\partial \zeta_3}{\partial x'} - \frac{\partial \xi_3}{\partial z}\right) + \frac{\partial \zeta_{\mathrm{TS}}}{\partial x'}\left(2\frac{\partial u_3}{\partial x'} + \frac{\partial v_3}{\partial y}\right) + \frac{\partial \zeta_{\mathrm{TS}}}{\partial y}\frac{\partial v_3}{\partial x'} + \frac{\partial^2 \zeta_{\mathrm{TS}}}{\partial x'^2}u_3 + \frac{\partial^2 \zeta_{\mathrm{TS}}}{\partial x'\,\partial y}v_3\right] - B\left[u_K\frac{\partial \nabla^2 v_3}{\partial x'} - \left(\frac{\partial^2 u_K}{\partial y^2} - \frac{\partial^2 u_K}{\partial z^2}\right)\frac{\partial v_3}{\partial x'} - 2\frac{\partial u_K}{\partial z}\frac{\partial \xi_3}{\partial x'} - 2\frac{\partial^2 u_K}{\partial y\,\partial z}\frac{\partial w_3}{\partial x'}\right] = \frac{\partial \nabla^2 v_3}{\partial t}, \tag{23}$$

with continuity

$$\frac{\partial u_3}{\partial x'} + \frac{\partial v_3}{\partial y} + \frac{\partial w_3}{\partial z} = 0. \tag{24}$$

We express the TS component of $\mathbf{v}_2$ as in Eq. (12), and α is the TS streamwise wave number. The streamfunction ψ_{TS} is dependent on the frequency parameter

$$F = 10^6\frac{\omega\nu}{U_\infty^2}$$

and on the displacement thickness Reynolds number, R_{δ_*}. The profile of ψ_{TS} is defined by a solution to the OS equation.

The Klebanoff streaks are expressed as

$$u_K(y,z) = u_K(y)\cos(\beta z), \tag{25}$$

where β is the characteristic spanwise wave number. The streak profile is given by the Squire response to an OS continuous mode, derived in Zaki and Durbin[11] (e.g., Fig. 1). The profile is given by the solution at a fixed time; however, the amplitude B will be treated as a parameter, so this analysis provides a shape. As we have noted previously, other studies have shown limited sensitivity to the streak *Ansatz*—we have perturbed our *Ansatz* and verified that observation.

The Floquet expansion for the problem (22)–(24) is

$$\mathbf{v}_3 = e^{\sigma t} \sum_{n=-\infty}^{\infty} \sum_{m=-\infty}^{\infty} \hat{\mathbf{v}}_{n,m}(y) e^{i[(n+\epsilon/2)\alpha x' + (m+\gamma/2)\beta z]}, \tag{26}$$

where ϵ and γ determine the classification of secondary instabilities and σ is the temporal eigenvalue.

It is clear that when $A=B=0$, Eq. (23) reduces to the OS equation and Eq. (22) reduces to Squire's equation. Solutions at different wave numbers are then fully decoupled, and the resulting eigenvalues should be the discrete and continuous modes for each wave number. The presence of a TS wave enables the interaction among all wave numbers in Eq. (26) with a given streamwise detuning factor ϵ [i.e., $\alpha\epsilon/2, \alpha(1\pm\epsilon/2), \alpha(2\pm\epsilon/2)\cdots$]. Similarly, the presence of a streak enables the interaction among all wave numbers with spanwise detuning by a factor γ.

E. Limitations of the proposed model

The new base flow (21) consists of a Blasius profile, a saturated TS wave, and a spanwise periodic streak. The *Ansatz* uses the local amplitude of the TS wave (A) and the local amplitude of the streak (B) as input parameters, which make it indirectly related to experiments such as the DNS of Liu *et al.*[6] In those simulations the input parameters are amplitudes of at the inlet (A_0 and B_0) and the response depends on their local amplitude after downstream evolution. The objective of the present analysis is not to relate secondary instability to an inlet condition, but rather to explain the mechanism underlying the instability itself.

III. NUMERICAL METHODS

A. Formulation details

Equations (22)–(24) with Eq. (26) and discretization in y provide an eigenvalue system of the form

$$\mathbf{A}\bar{x} = \sigma \mathbf{B}\bar{x}, \tag{27}$$

where $\mathbf{A}$ is a matrix operator representing terms on the left hand sides and $\mathbf{B}$ the terms on the right hand side. The eigenvector $\bar{x}$ is the velocity vector $(\bar{u},\bar{v},\bar{w})^T$ and σ is the complex eigenvalue defined in Eq. (26). In computations, a real Fourier expansion, rather than the complex expansion shown in Eq. (26), is used for convenience.

B. Algorithmic implementation

Equations (22)–(24) can only be solved numerically. The core of a numerical solution is the generation of matrices $\mathbf{A}$ and $\mathbf{B}$ of Eq. (27). The interaction among streamwise wave numbers and also among spanwise wave numbers in the doubly periodic Floquet expansion reduces the sparsity of matrices $\mathbf{A}$ and $\mathbf{B}$. By substituting the Floquet expansion (16) into the governing equations, Eqs. (22) and (23), and calculating the convolution terms explicitly, one can obtain governing equations for each mode. By grouping terms, formulas can be derived for each entry of the matrix of the eigensystem. The resulting formulas are, however, extremely complicated and involve hundreds of terms. As a result, the derivation of these expressions is prone to errors, whether performed manually or with symbolic manipulation programs, such as MATHEMATICA. The numerical implementation is an equally cumbersome procedure and can introduce further inaccuracies. The complexity of the formulas increases dramatically when more Fourier components are included or when additional terms are added in the governing equations. A different approach is therefore adopted and will be summarized below, but first we present an example of the structure of the eigenvector $\bar{x}$ in Eq. (27).

Consider fundamental modes in both directions and truncate the expansion at the second Fourier mode. Then the eigenvector takes the form

$$\bar{x} = (\bar{u}_{0,0}, \bar{u}_{\alpha,0}, \bar{u}_{2\alpha,0}, \bar{u}_{0,\beta}, \bar{u}_{\alpha,\beta}, \bar{u}_{2\alpha,\beta}, \bar{u}_{0,2\beta}, \bar{u}_{\alpha,2\beta}, \bar{u}_{2\alpha,2\beta})^T, \tag{28}$$

where α is the fundamental streamwise wave number and β is the fundamental spanwise wave number. Each velocity vector at a specific wave number has three components,

$$\bar{u}_{\alpha,\beta} = (u_{\alpha,\beta}, v_{\alpha,\beta}, w_{\alpha,\beta})^T, \tag{29}$$

and each velocity component has Fourier terms of the form

$$u_{\alpha,\beta} = (u^1_{\cos(\alpha)\cos(\beta)}, u^2_{\sin(\alpha)\cos(\beta)}, u^3_{\cos(\alpha)\sin(\beta)}, u^4_{\sin(\alpha)\sin(\beta)})^T. \tag{30}$$

Suppose N collocation points in y are used for each velocity in Eq. (30), N_A Fourier components are retained in the streamwise direction, and N_B are retained in the spanwise direction. Let Z_A and Z_B take the value of 1 if the expansions in the respective directions include the zero-frequency mode, otherwise they are 0. The length of the eigenvector $\bar{x}$ is found to be

$$M = (4N\times 3\times N_A + 2N\times 3\times Z_A)N_B + (2N\times 3\times N_A + N\times 3\times Z_A)Z_B. \tag{31}$$

In the above example, where $N_A=N_B=2$ and $Z_A=Z_B=1$, the sizes of the eigenvector are 2250 if $N=30$ and 3750 if $N=50$. The matrices $\mathbf{A}$ and $\mathbf{B}$ are of the size $(M\times M)$, which can become extremely large.

In order to avoid deriving explicit formulas for such large matrices, we adopt an alternative approach. The basic idea is to numerically implement Eqs. (22)–(24) as they appear, in operator form, rather than by deriving expressions for each wave number vector. For every term in the governing equation (e.g., $Bu_K \partial\eta_3/\partial x'$), a call to a template function identifies an operand (η_3), operator ($\partial/\partial x'$), and scaling vector (Bu_K). The template function automatically generates the necessary instructions to construct the operand from the elementary variables (u,v,w) to compute the Floquet expansion and to evaluate any required convolution terms. It then calls a locator routine which adds the resulting terms to the appropriate entries in the matrices $\mathbf{A}$ and $\mathbf{B}$. In this framework, once the elementary operators are created, complex expressions can be constructed automatically, without error. The final expression (27) remains identical to the conventional approach of deriving governing equations for every wave number pair. The resulting eigensystem is solved by a general complex eigenvalue solver from the NAG library.

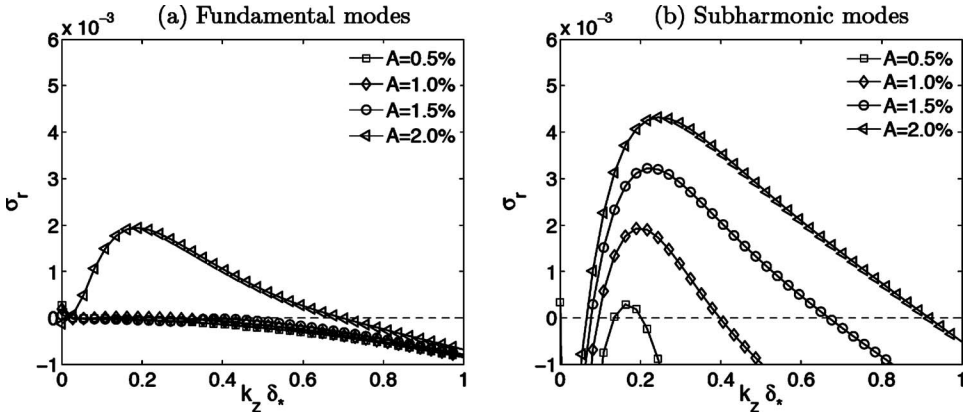

FIG. 4. Secondary instability of a boundary layer distorted by two-dimensional TS waves. Growth rates of both the streamwise (a) fundamental and (b) subharmonic Floquet modes are plotted vs the spanwise wave number.

The implementation and numerical solution to the eigenvalue problem is validated using established results from the literature in Appendix.

Before we discuss the instability of the Blasius profile when distorted by both the TS waves and streaks, in Secs. IV and V, we consider the stability of a base state which is only periodic in one direction. These results establish the influence of the primary TS wave or streak distortion, when each is acting alone, on the stability of the boundary layer. These results are followed by a discussion of the stability of the boundary layer when both components are present.

IV. SECONDARY INSTABILITY OF THE PRIMARY TS WAVE

In the DNS of Liu *et al.*,[6] when a primary TS wave with reduced frequency $F=120$ was applied alone at the inlet, it amplified downstream. The amplification of the primary wave is consistent with a supercritical inlet Reynolds number where, based on the inflow boundary layer displacement thickness and free-stream velocity, $R_{\delta_*}=688$. Although this Reynolds number is at the inlet to the computational domain, it will be retained for the saturated TS wave in the Floquet analysis. Secondary instability was not observed within the computational domain, which was attributed to the absence of any appreciable level of noise in the DNSs.

A Floquet analysis of the stability of this flow, composed of a Blasius state distorted by a two-dimensional primary TS wave, yields similar observations to Herbert.[15] The results are summarized here, and are in later sections contrasted to the secondary instability when the streaks are also included. Figure 4 displays the growth rate of the three-dimensional secondary instabilities of the TS waves as a function of the spanwise wave number of the instability. Both the streamwise fundamental (left pane) and subharmonic (right pane) modes were considered. The results demonstrate that the streamwise subharmonic mode is most unstable. This assertion is further verified by computing the maximum growth rate of the secondary instability at $k_z\delta_*=0.54$ over the range of the detune factor ϵ (Fig. 5); indeed the subharmonic instability is most pronounced when $A>0.02$ in that figure.

In Fig. 4, the maximum amplification of secondary modes is at $k_z\delta_*\sim 0.19-0.22$, which is equivalent to a wavelength of over ten boundary layer thicknesses. This optimal spanwise size should match that of the Λ-structures, where they to develop from broadband, background perturbations. It is interesting to note that this size is much larger, by nearly an order of magnitude, than the instabilities computed in subsequent sections and observed in the DNS of Liu *et al.*[6] when Klebanoff streaks are present. This indicates that the size of the Λ-structures seen in DNS (e.g., Fig. 3) is in part affected by the Klebanoff distortion of the base flow—rather than the maximum secondary instability of a TS waves *per se*.

Another observation from Fig. 4 is that the three-dimensional secondary eigenmodes are stable for spanwise wave numbers $k_z\delta_*\geq 1$ and $A\leq 2\%$ of the free-stream velocity. This result does not take into account any streaks and is also expected to change in the doubly periodic analysis: In the DNS of Liu *et al.*,[6] when streaks are present, secondary instabilities were observed at higher spanwise wave numbers, $k_z\delta_*\geq 1$, even at lower amplitude of the primary TS waves. In short, the Λ-structures which develop in the presence of streaks do not exist in Herbert's framework. Their very presence must be related to the influence of boundary layer streaks.

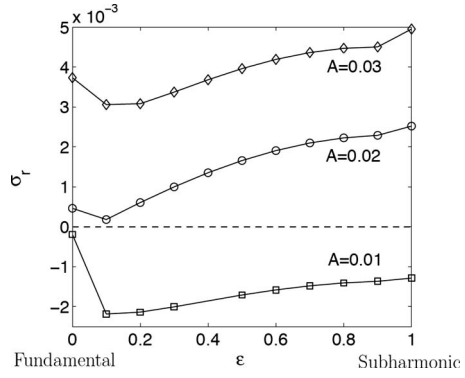

FIG. 5. Secondary instability of a boundary layer distorted by two-dimensional TS waves. The growth rate is evaluated for a three-dimensional instability wave, $k_z\delta_*=0.54$, over the range of the streamwise detuning factor ϵ.

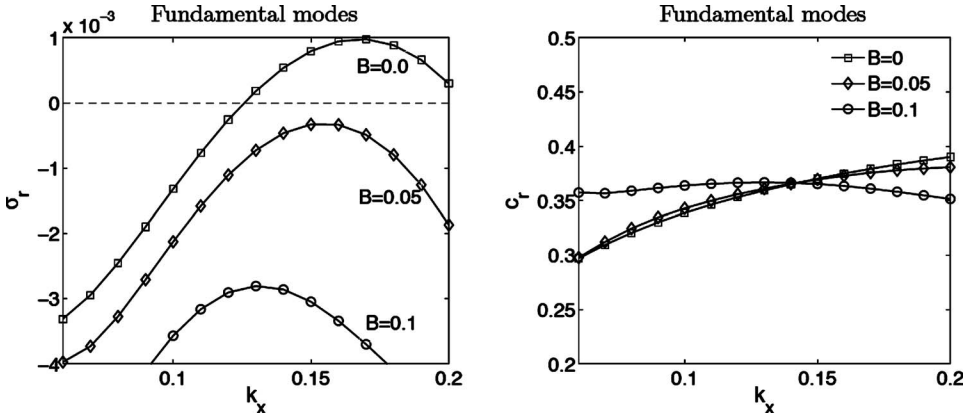

FIG. 6. Growth rate σ_r and phase speed c_r of the secondary instability of a boundary layer distorted by streaks of spanwise size, $\beta\delta_*=0.54$ (mode 2). The spanwise fundamental Floquet mode is shown; the computed instability has its origin in the two-dimensional TS wave at zero streak amplitude.

V. STABILITY OF A BLASIUS BOUNDARY LAYER DISTORTED BY KLEBANOFF STREAKS

The discrete TS waves of a simple Blasius boundary layer are often referred to as primary instability modes. Here we consider a base flow which is the Blasius profile distorted by Klebanoff streaks. Discrete instability waves of this base state exist and can be traced back to the primary TS waves as the streak amplitude is reduced. Therefore, these instabilities can be regarded as modified TS waves of a Klebanoff-distorted boundary layer. When the instability has its root in a two-dimensional TS wave, it is dominated by the zeroth spanwise mode in the spanwise Floquet expansion, but will also include contributions from harmonics of the streak spanwise wave number.

In our analysis, we use the solution to the Squire initial value problem in order to represent the streaks. The instability of the Balsius boundary layer distorted only by the Squire streaks was computed, and a similar behavior to Cossu and Brandt[13] was observed. Figure 6 shows the growth rate of the computed TS-type waves versus their streamwise wave number in the presence of streaks at various amplitudes. The observed reduction in the growth rate is significant. The wave speed of these disturbances is also shown and is commensurate with the result for a TS instability of a Blasius profile.

The results in Fig. 6 describe the dependence of the TS-type instability on a streak of a particular spanwise size, $\beta\delta_*=0.54$ (mode 2). The analysis was repeated for a number of spanwise sizes of the streak and is shown in Fig. 7. In the regime $\beta\delta_*>0.5$, the dependence of the growth rate on wave number is less pronounced than the dependence on the streak amplitude.

The stabilizing influence of the streaks on the TS-type instabilities of the boundary layer is important in the context of the simulations of Liu *et al.*[6] In those simulations, both primary TS waves and streaks were prescribed at the inflow of the computational domain. Since the streaks are long in the streamwise extent, the superposition of the streak and the Blasius profile presents in effect a new base flow for the primary TS wave. Indeed, the growth rate of the primary TS wave was observed to decrease with increasing streak amplitude in the DNS. This is consistent with the current analysis which, in a sense, describes the early stages of the flow evolution in the DNS.

Farther downstream, a secondary instability of the primary TS waves was observed in the simulations. That instability was not independent of the streaks. Therefore, in Secs. VI and VII we discuss the results of the secondary instability problem when the base flow is a superposition of the Blasius profile and both a primary TS wave and a Klebanoff distortion.

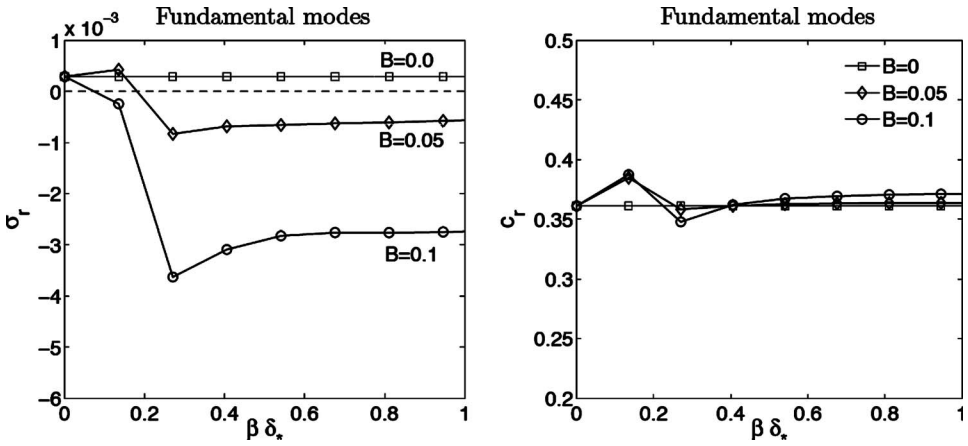

FIG. 7. Growth rate σ_r and phase speed c_r of the secondary instability of a boundary layer distorted by streaks of various spanwise sizes. The computed instability has its origin in the two-dimensional TS wave at zero streak amplitude.

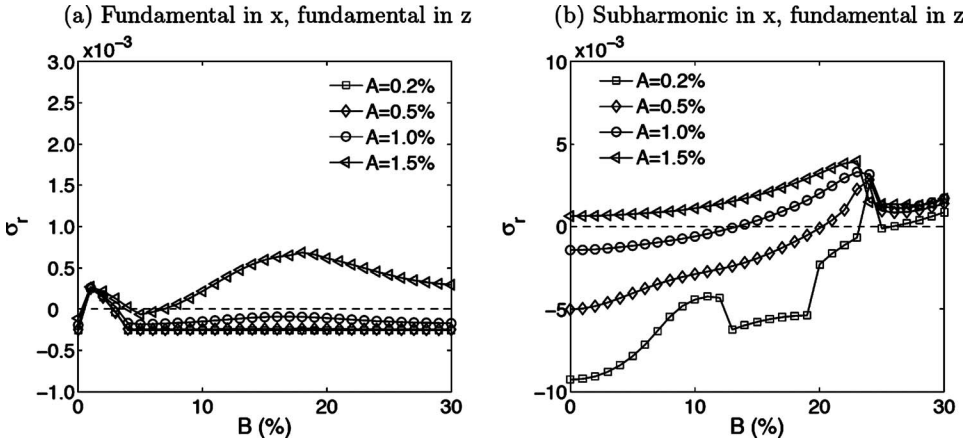

FIG. 8. Effect of the streak strength B on the growth rate σ_r of the secondary instability. The fundamental and subharmonic modes in x are shown, both assuming a spanwise expansion in terms of the fundamental streak wave number (mode 2, $\beta\delta_*=0.54$).

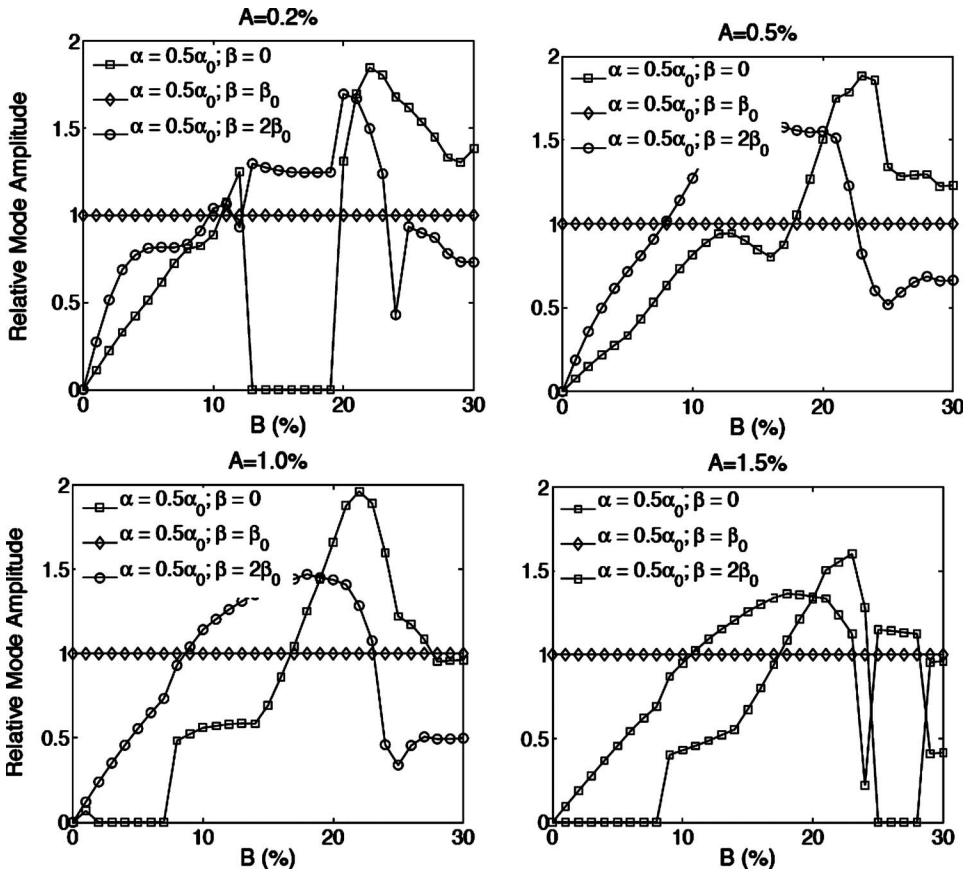

FIG. 9. Relative strength of the Fourier components in the Floquet analysis of Fig. 8(b). The change of the dominant Fourier mode causes the sharp changes in the growth rate curve.

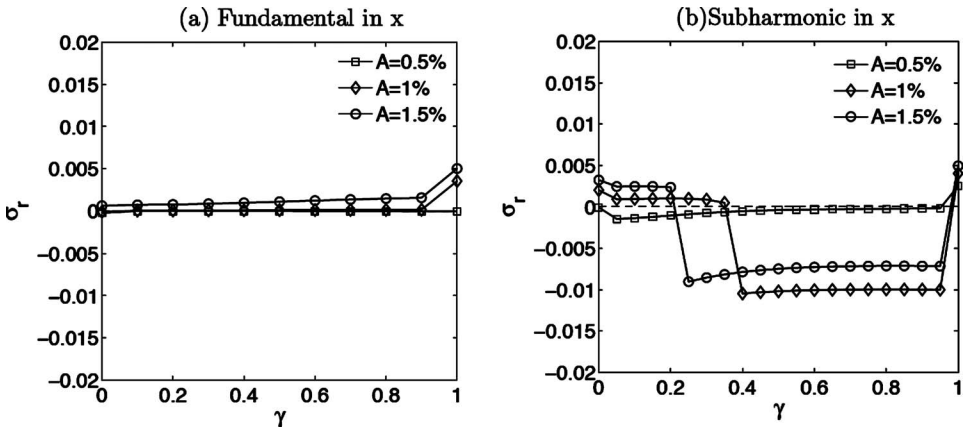

FIG. 10. Effect of γ on the growth rate σ_r of the streamwise fundamental and subharmonic instability of wide streaks (mode 2, $\beta\delta_*=0.54$). The streak amplitude, $B=20\%$, is representative of the maximum intensity recorded in the simulation of Liu *et al.* (Ref. 6).

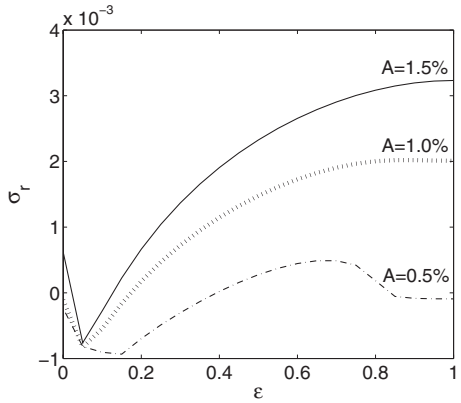

FIG. 11. Effect of the streamwise detune factor ϵ on the growth rate of the secondary instability for wide streaks (mode 2, $\beta\delta_*=0.54$). The streak amplitude is 20%.

VI. THE INFLUENCE OF WIDE STREAKS ON SECONDARY INSTABILITY

When both the discrete and continuous modes are present in the flow, the secondary instability problem requires a Floquet expansion in two directions. We will identify Floquet modes by the two detuning factors ϵ and γ. As explained in Sec. II, fundamental modes have a detuning factor of 0 and subharmonic modes have a detuning factor of 1. A mode with $\epsilon=1$ and $\gamma=0$ is referred to as subharmonic in x and fundamental in z.

Let us start by noting a DNS result of Liu *et al.*[6] When both the continuous mode, $\beta\delta_*=0.54$ (mode 2), and the TS wave were included at the inflow, the maximum recorded streak amplitude was 21% of the free-stream velocity. Breakdown of the boundary layer was preceded by the formation of Λ-structures that matched the continuous mode spanwise wavelength (Fig. 2). In addition, an increase in the amplitude of the inlet continuous mode caused transition to move upstream.

In those simulations, the inflow included unsteadiness at the Klebanoff streak wavelength. This acts as an unsteady perturbation which can promote secondary instability. Thus disturbances which are fundamental in z ($\gamma=0$) should be provoked, if they have positive growth rate. This is investigated using our Floquet analysis. The growth rate of the eigenmodes that are fundamental in z is plotted in Fig. 8 versus the streak amplitude. Both the fundamental and subharmonic expansions in x are shown, and the latter has a larger growth rate. The fundamental instability in z explains the spanwise size of the Λ-structures which appear in the DNS, and which match the width of the streaks. It should also be noted that the growth rate of the secondary instability which is subharmonic in x and fundamental in z [Fig. 8(b)] increases nearly monotonically with increasing streak amplitude. This is consistent with the DNS result that transition moved upstream with amplitude of the wide streak (mode 2, $\beta\delta_*=0.54$).

For a TS wave with local amplitude of 1%, the secondary disturbances become unstable only when $B>13\%$. For smaller B, the primary TS waves initially grow more slowly than when $B=0$ and may even decay. But Klebanoff streaks grow relatively quickly, so that a stage of high streak intensity and moderate TS amplitude develops. At this stage, secondary instability sets in. Indeed, that is what is observed in the DNS: the streaks cause a quick transition, shortly downstream from the inlet. The spanwise spacing of Λ-structures is the same as the streak spanwise wavelength.

The dependence of the secondary instability on the amplitude of the primary TS wave is also shown in Fig. 8. The results indicate that the "window" of instability narrows at lower amplitudes of the primary wave. As a result, transition is less likely at lower TS amplitudes.

Figure 9 shows the relative strength of the Fourier components of the perturbation which is subharmonic in x and fundamental in z [Fig. 8(b)]. The wall-normal maximum of each component in the Floquet expansion, normalized by $u^{\max}_{\alpha,\beta}$, is plotted versus streak amplitude [see Eq. (28)]. Sharp turns in Fig. 8(b) are the result of changes in the dominant Fourier component. Since the curves in Figs. 8 and 9 are not smooth, a resolution test was performed:[5] these results appear to be independent of the grid size.

The existence of a spanwise fundamental instability has now been established. However, evidence in the literature suggests that long-wavelength spanwise modulation of the mean flow can lead to fundamental and subharmonic instabilities, with the later showing higher growth rate.[16,17] This observation was made, for instance, by Li and Malik,[17] in the context of modulation of the mean flow by steady Görtler vortices. Therefore, we evaluate the influence of the span-

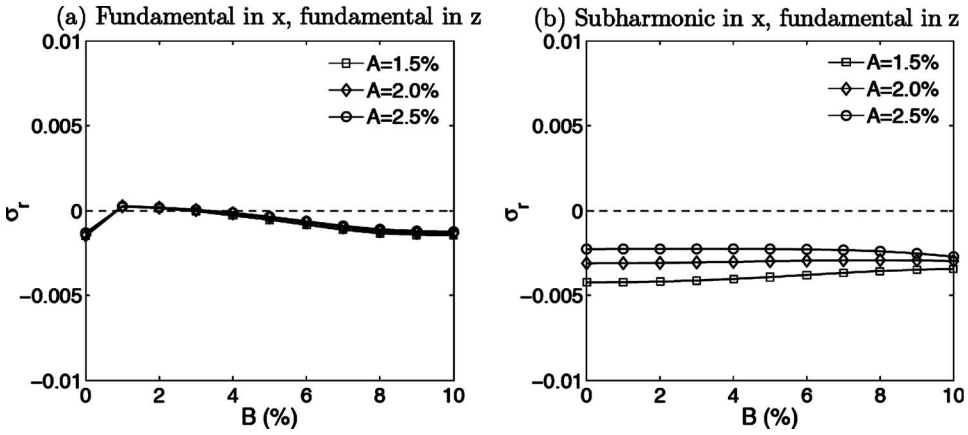

FIG. 12. Effect of the streak strength B on the growth rate σ_r of the streamwise (a) fundamental and (b) subharmonic instabilities, both assuming a fundamental spanwise expansion in wave number of the narrow streaks (mode 5, $\beta\delta_*=1.35$).

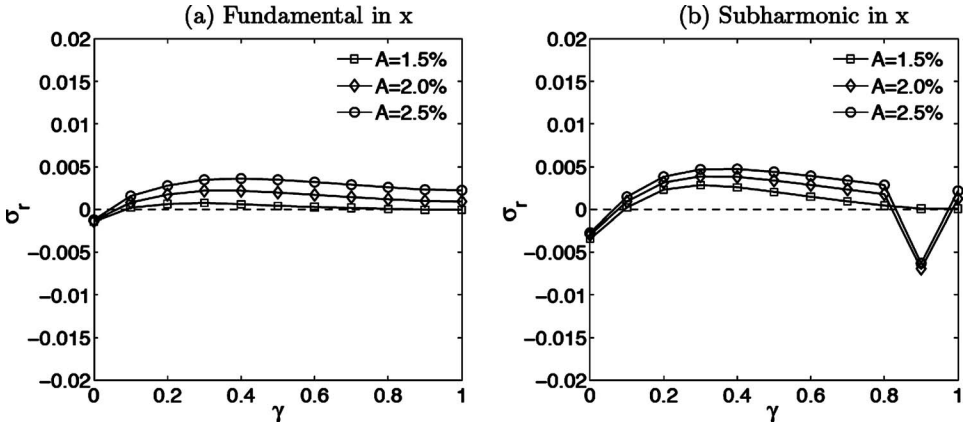

FIG. 13. Effect of the detune factor γ on the growth rate of the streamwise (a) fundamental and (b) subharmonic instabilities. The streak spanwise wave number is $\beta\delta_*=1.35$ (mode 5). The streak amplitude $B=10\%$ is representative of the simulation of Liu *et al.* (Ref. 6).

wise detune factor γ in Fig. 10. Indeed the spanwise subharmonic mode is slightly more unstable than the fundamental.

Since both the spanwise fundamental and subharmonic modes are unstable (Fig. 10), both can emerge in the fully nonlinear simulations. The dominant instability in the DNS is, however, dependent on the perturbations that are present in the flow, and which excite the secondary instability. In the DNS of Liu *et al.*,[6] the inlet perturbation includes unsteadiness only at the fundamental spanwise wavelength. The spanwise subharmonic was absent upstream of transition in the simulations. Due to this forcing at the fundamental wave number, the Λ-structures were seen to acquire the spanwise size of the streaks.

While the width of the Λ-structures which emerge in the DNS is explained in terms of the spanwise fundamental instability, their streamwise pattern is more complex. The paired and staggered arrangements observed in the DNS displayed a periodicity at four times the wavelength of the primary TS wave (see Fig. 2). This corresponds to a streamwise detune factor, $\epsilon=1/2$. The influence of ϵ on the growth rate of the secondary instability was computed using our Floquet algorithm, and is shown in Fig. 11. The results demonstrate that the optimal detune factor in x is $\epsilon\sim 0.7$ for $A=0.5\%$ and it shifts toward the subharmonic at higher TS wave amplitudes. This provides an explanation of the streamwise periodicity of the Λ-structures which emerge in the DNS of Liu *et al.*[6]

However, it also should be noted that the continuous modes were unsteady in the simulations, which causes the direction of the perturbation jets to oscillate with time. This may cause the staggering directly.[6]

VII. THE INFLUENCE OF NARROW STREAKS ON SECONDARY INSTABILITY

The narrow streak case has $\beta\delta_*=1.35$ (mode 5). Breakdown of the boundary layer in the presence of TS waves and narrow streaks proceeded in a manner quite distinct from that discussed in Sec. VI. In the DNS,[6] the onset of transition is delayed as the streak amplitude increased. In addition, the Λ-structures had a spanwise size different from that of the streaks. Again, Floquet theory offers an explanation.

Figure 12 shows the growth rate of secondary instability modes that are fundamental in z. If these modes were to possess positive growth rates, they would be favored. They are all, however, decaying. Although the fundamental modes are slightly unstable under very weak streaks, this period is short lived in the DNS where the streaks amplify quickly downstream of the inlet plane (in the linear limit, the solution of the OS-Squire initial value problem shows that the ampli-

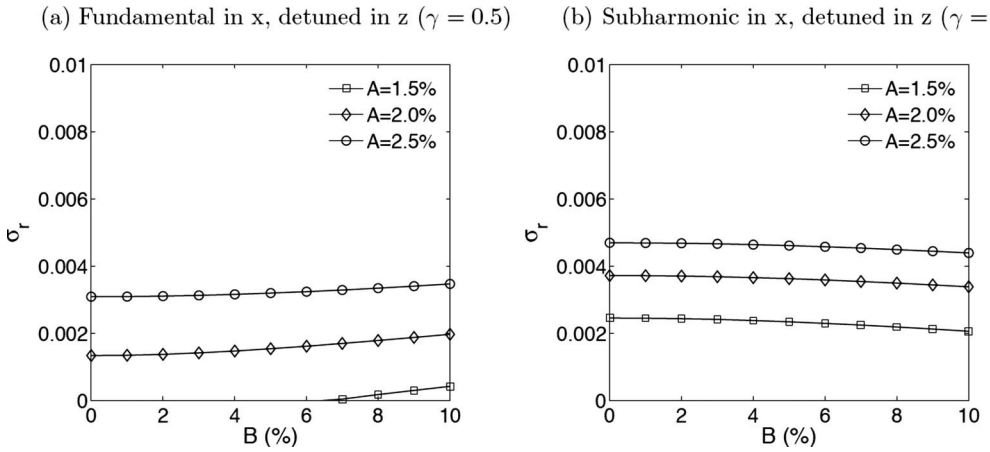

FIG. 14. Effect of the streak strength B on the growth rate of the streamwise fundamental and subharmonic instabilities in the presence of narrow streaks, $\beta\delta_*=1.35$ (mode 5). The spanwise detune factor, $\gamma=0.5$.

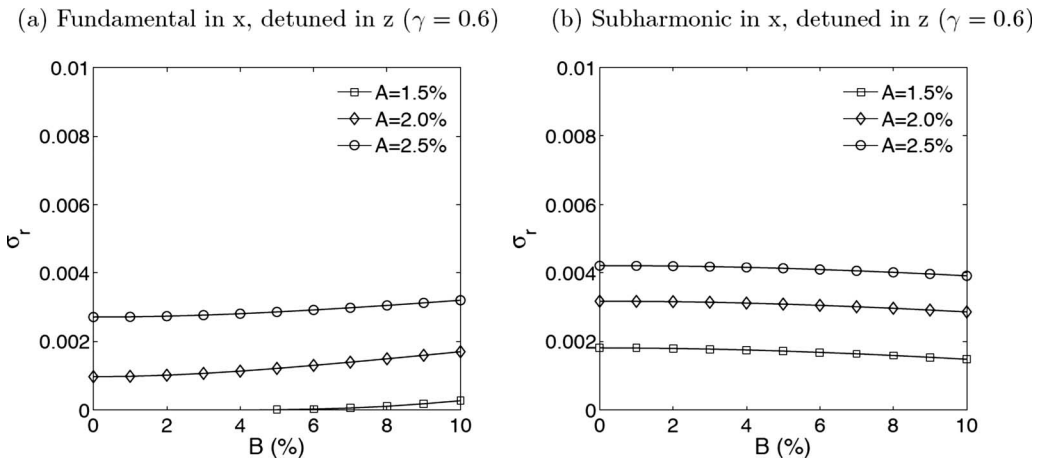

FIG. 15. Effect of the streak strength B on the growth rate of the streamwise fundamental and subharmonic instabilities in the presence of narrow streaks, $\beta\delta_*=1.35$ (mode 5). The spanwise detune factor, $\gamma=0.6$.

tude of the streaks grows linearly in time[11]). As a result, the instability at low values of B does not contribute significantly to the development of the secondary instability.

A study of the effect of the spanwise detune factor γ is shown in Fig. 13. Unlike the wide streaks, which are dominated by their fundamental and subharmonic instability, the maximum growth rate in Fig. 13 occurs at $\gamma\sim0.4$, and the curve is quite flat in the interval $0.3<\gamma<0.7$. The Λ-structures observed in DNS correspond to $0.5\leq\gamma\leq0.67$, which is within the range of secondary instability predicted by our analysis. It is also important to note that this spanwise size of the secondary instability wave is appreciably smaller than the Herbert type, which was evaluated in Sec. IV in the absence of streaks. Therefore, the computed secondary instability is influenced by the spanwise periodicity of the Klebanoff distortion, despite not directly matching the streak width.

Figures 14 and 15 display the growth rate of two modes in the range of $0.3<\gamma<0.7$ evaluated as a function of streak amplitude. The amplification rate is fairly insensitive to streak amplitude. Increasing B does not enhance the secondary instability; it only suppresses the growth rate of the primary TS wave according to the analysis of Sec. V. This provides an explanation for why larger streak amplitude was seen to delay transition in DNS.

The simulations of Liu *et al.*[6] produced slower transition to turbulence in the presence of narrow streaks, $\beta\delta_*=1.35$ (mode 5), than in the presence of wide streaks, $\beta\delta_*=0.54$ (mode 2): secondary instability emerged farther downstream and transition took place at higher Reynolds numbers. This is partly because the secondary instability is weakly dependent on the streak amplitude (see Fig. 12). Instead, a stronger TS wave is required in order to obtain a significant secondary instability. The requirement for greater amplification of the primary TS wave prior to instability is, in part, responsible for a downstream shift in the transition location. Another reason, potentially of more importance, is that the spanwise wave number of the inlet continuous mode does not match the wave number of the detuned secondary instability. Energy transfer from the streak wave number to that of the Λ-structures is therefore not supported directly. In the DNS, nonlinearity creates a broader spectrum of wave numbers to trigger detuned instabilities.

VIII. DISCUSSION

Transition by interaction of TS waves and streaks can proceed in different manners, depending on the spanwise wave number of the latter. Both wide and narrow streaks have a stabilizing effect on the primary TS wave. Their effect on the secondary instability is, however, distinct. In the wide streak case (mode 2, $\beta\delta_*=0.54$), the Floquet analysis predicts both fundamental and subharmonic secondary instabilities. The former, despite a slightly smaller growth rate, is favored in the DNS due to the unsteady inflow perturbation. In the narrow streak case (mode 5, $\beta\delta_*=1.35$), the fundamental spanwise mode is stable; instead, detuned modes are unstable (Fig. 13). The Floquet result therefore explains why transition occurred in the DNS via Λ-structures corresponding to a detune factor, $\gamma\sim0.5$.

Another difference between the wide and narrow streaks considered thus far is the effect of increasing the streak am-

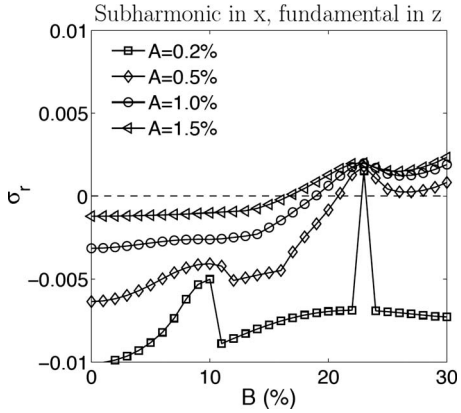

FIG. 16. Secondary instability in the presence of TS waves and streaks of spanwise wave number, $\beta\delta_*=0.81$ (mode 3). The effect of the streak strength B on the growth rate σ_r of the streamwise subharmonic and spanwise fundamental instabilities.

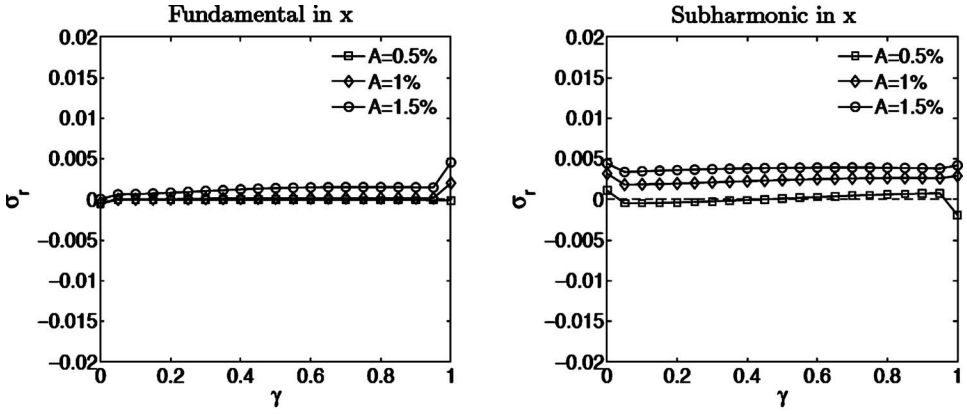

(a) Mode 1, $\beta\delta_* = 0.27$, $B = 20\%$.

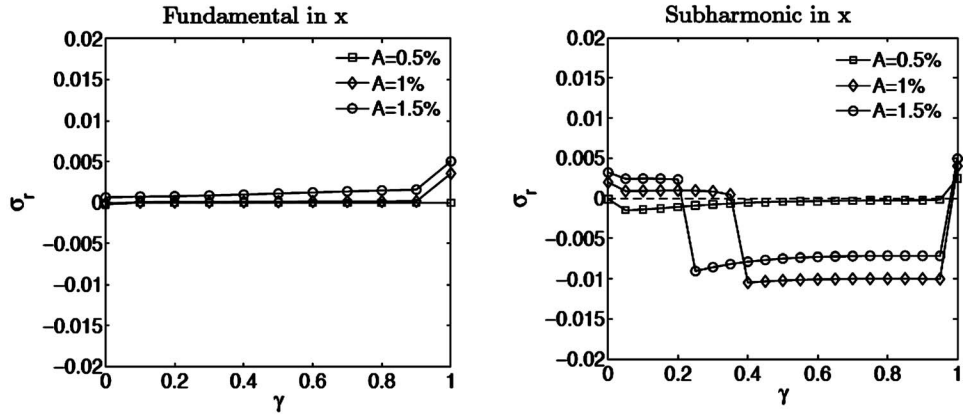

(b) Mode 2, $\beta\delta_* = 0.54$, $B = 20\%$.

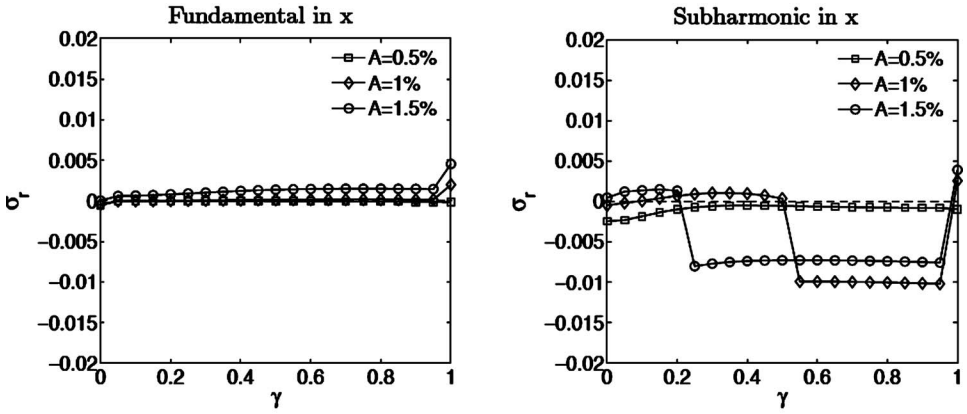

(c) Mode 3, $\beta\delta_* = 0.81$, $B = 18\%$.

FIG. 17. Effect of γ on the growth rate of the streamwise fundamental and subharmonic secondary instabilities. Values of γ correspond to instability modes with $k_z=(\gamma/2)\beta$, $(1\pm\gamma/2)\beta$, etc.

plitude. In the former, transition moves upstream and, in the latter, transition is delayed. In the case of wide streaks, increasing the streak amplitude has the dual role of stabilizing the primary TS wave, and also *increasing* the growth rate of that fundamental instability (Fig. 10)—the net balance is early transition. On the other hand, higher amplitude narrow streaks stabilize the primary TS wave, but do not affect the growth rate of the detuned secondary instability (Figs. 15 and 14)—the net effect is therefore transition delay.

A natural question arises: how does the transition pattern change as the spanwise wave number is varied gradually. In the study of Liu *et al.*,[6] transition did not take place when a continuous mode with $\beta\delta_*=0.8$ (mode 3) and $B_0=2.1\%$ was included at the inflow. However, for lower amplitude ($B_0=1\%$), breakdown was observed, preceded by Λ-structures of the same size as the streaks. The maximum streak amplitude in these simulations was $B=18\%$. Figure 16 explains why transition in this case is difficult to realize. According to the Floquet analysis, when $B=18\%$, the secondary eigendisturbances are only unstable for large amplitudes of the pri-

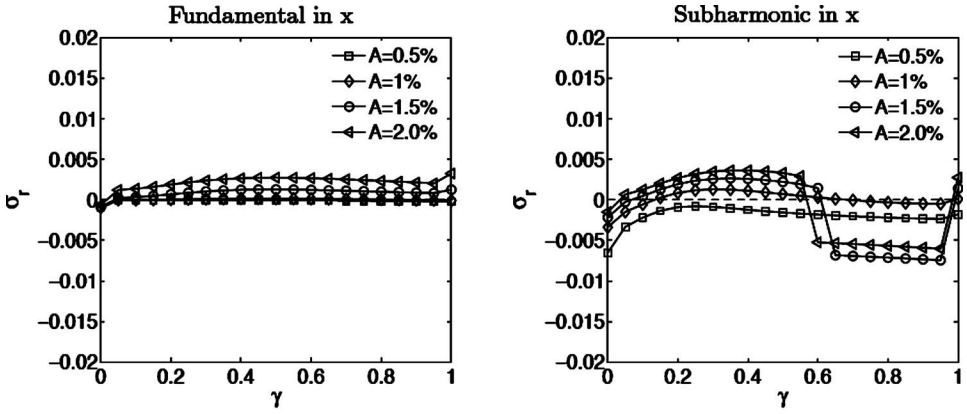

(d) Mode 4, $\beta\delta_* = 1.08$, $B = 14\%$.

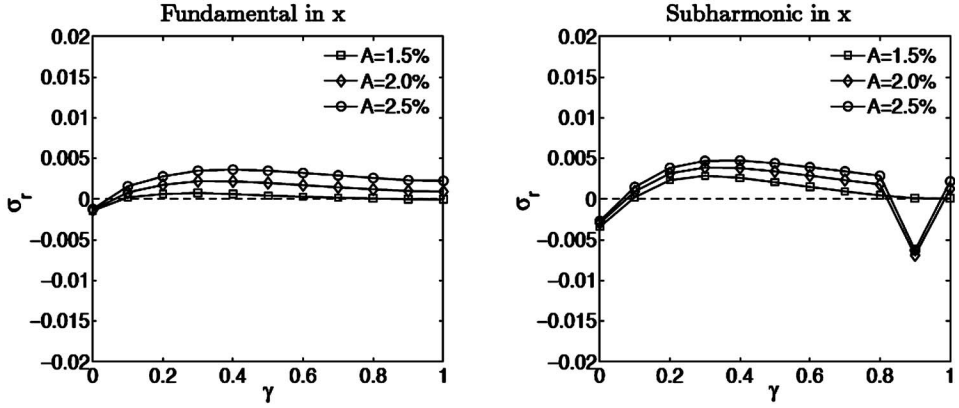

(e) Mode 5, $\beta\delta_* = 1.35$, $B = 10\%$.

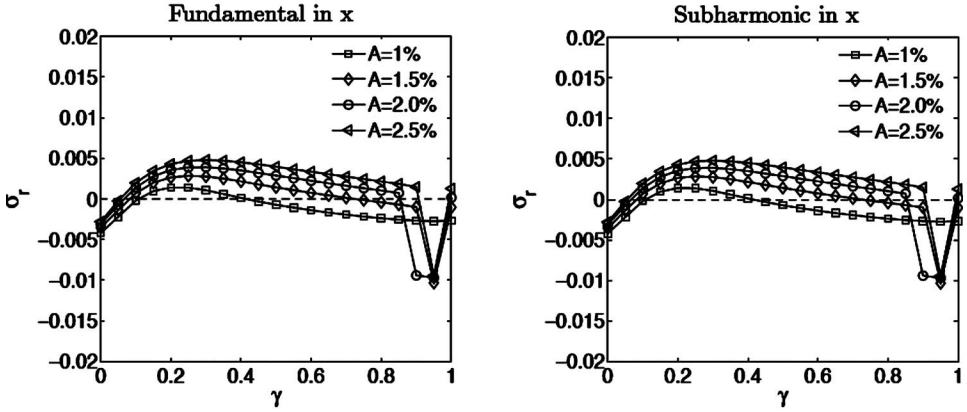

(f) Mode 6, $\beta\delta_* = 1.62$, $B = 10\%$.

FIG. 18. Effect of γ on the growth rate of the streamwise fundamental and subharmonic secondary instabilities, continued.

mary TS waves, $A > 1\%$. However, strong streaks suppress the primary TS waves. Only weaker Klebanoff streaks, which do not suppress the growth of TS waves significantly, permit them to grow to a critical amplitude for transition.

Figures 17 and 18 explain how the transition pattern changes with the spanwise wave number of the Klebanoff streaks. In these figures, the amplitudes of the streaks are reduced as their spanwise wave number increases. This reduction in amplitude is due to the following reason: given an initial v-eigenperturbation, the maximum amplitude of the induced streaks depends on the spanwise wave number of the forcing. At higher values of β, this maximum amplitude of the streaks is reduced due to viscous dissipation. This reduction in maximum amplitude is accounted for in the figure.

The continuous modes $\beta\delta_* = \{0.27, 0.54, 0.81\}$ (modes 1–3) cause a secondary instability at their fundamental spanwise wavelength ($\gamma = 0$). The growth rate of the fundamental frequency becomes negative when $\beta\delta_* > 1.08$ (>mode 4) and detuned modes, $\gamma \sim 0.3-0.4$, become most unstable. As a result, transition for streaks of spanwise wave number $\beta\delta_* = \{1.08, 1.35, 1.62\}$ (modes 4–6) takes place at spanwise detuned wavelengths. This mechanism is usually slower than

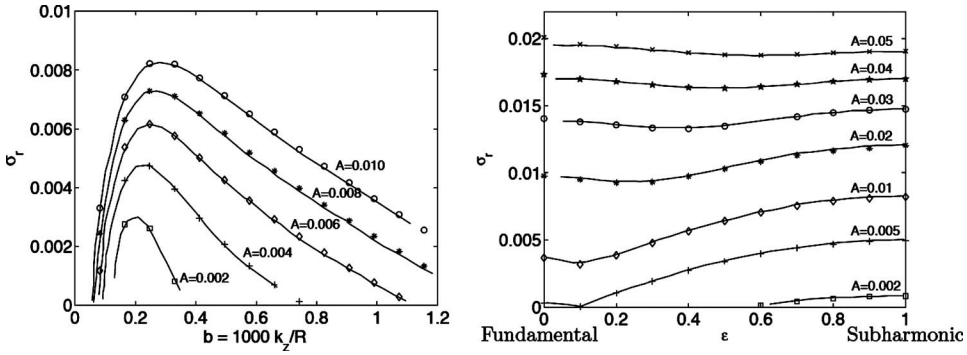

FIG. 19. Validation vs results from Herbert (Ref. 7) at $R_{\delta_*}=1042$, $F=124$. At left, growth rate of the subharmonic, $\epsilon=1$, secondary instability mode as a function of the spanwise wave number. At right, the growth rate is plotted vs the detuning factor at $k_z=0.2$. Symbols are current results and lines are obtained from Ref. 7.

breakdown via fundamental resonance which exactly matches the strong forcing by the inflow continuous mode disturbance.

In cases where the secondary instability occurs at the fundamental spanwise wavelength of the streaks, increasing the amplitude of the streaks generally promotes breakdown. But transition can be suppressed if the inflow primary TS mode is too weak or is excessively attenuated by strong streaks. This behavior is most likely in the case of detuned resonance: When the inlet perturbation does not match the spanwise wavelength of secondary instability, large amplitude streaks can significantly attenuate the primary TS wave prior to the nonlinear cascade of energy to unstable wave numbers. As a result, increasing the streak amplitude in detuned resonance generally delays transition.

ACKNOWLEDGMENTS

We are grateful to Professor Vassilis Theofilis, who provided his Floquet code as a starting point for our work.

APPENDIX: VALIDATION OF THE DOUBLY PERIODIC FLOQUET ALGORITHM

The secondary instability equations (22)–(24) were discretized in the manner described in Sec. III, leading to the eigenvalue problem

$$\mathbf{A}\bar{x}=\sigma\mathbf{B}\bar{x}. \tag{A1}$$

The discretized eigensystem (A1) accounts for the periodicity of the base flow in the streamwise and spanwise directions due to two-dimensional TS waves and streaks, respectively.

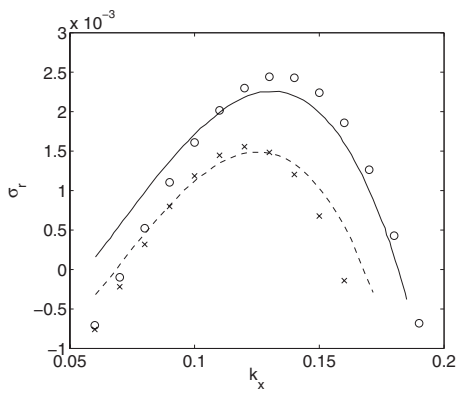

FIG. 20. Growth rate σ_r of the modified TS wave of a boundary layer distorted by streaks at $R_{\delta^*}=1,934$. The streak spanwise wave number is $k_z\delta^*=0.774$. Two streak amplitudes are shown: (—) $B=0$; (– – –) $B=14\%$.

The validation of the numerical, doubly periodic Floquet expansion is carried out in two steps: First, the implementation of the streamwise expansion is validated against Herbert,[7] where the base flow is a Blasius boundary layer and a two-dimensional TS wave. Second, the validation of the spanwise expansion is performed by comparing our results to Cossu and Brandt,[13] who studied the instability of a base flow composed of a Blasius boundary layer and spanwise streaks. The validation using two unidirectional periodic cases is sufficient because the doubly periodic base flow has the form

$$\mathbf{v}_2(y,z,t)=U_0(y)\vec{e_x}+A[u_{\mathrm{TS}}(x',y)\vec{e_x}+v_{\mathrm{TS}}(x',y)\vec{e_y}]+Bu_K(y,z)\vec{e_x}, \tag{A2}$$

where every term in the superposition is at most periodic in one direction, and the problem is linear.

The comparison to Herbert[7,15] is shown in Fig. 19. The secondary instability of two-dimensional TS waves was computed at the same base-flow conditions of that paper, $R_{\delta_*}=1042$, $F=124$. These parameters place the primary TS wave on the upper branch of the neutral stability curve. The plot at left shows the growth rate of the streamwise subharmonic secondary instability ($\epsilon=1$) versus its spanwise wave number. At right, the growth rate is plotted versus the streamwise detune factor for a particular spanwise wave number of the secondary instability mode. Good quantitative agreement is observed between our results (symbols) and those of Herbert[7] (lines).

TABLE I. Effect of the streak amplitude on the growth rate and wave speed of the most unstable mode.

	Cossu and Brandt[a]		Current results	
Streak amplitude B	σ_r ($\times 10^3$)	c_r	σ_r ($\times 10^3$)	c_r
0%	2.258	0.3209	2.442	0.3122
14.0%	1.485	0.3144	1.473	0.3207
20.0%	0.652	0.3084	0.6122	0.2752
24.3%	−0.131	0.3046	0.1088	0.2564

[a]Reference 13.

A comparison of our numerical Floquet results to Cossu and Brandt[13] is shown in Fig. 20 and Table I. The base flow is a superposition of a Blasius profile and a steady Klebanoff streak, and is therefore periodic only in the span. The Floquet analysis yields the instability mode which has its origin in the conventional, "primary" TS wave. Because streaks are modeled differently here and in Cossu and Brandt,[13] an exact comparison was not possible. However, reasonably accurate agreement was obtained by matching the amplitude and spanwise wave number of the base-flow streaks.

The results of Cossu and Brandt[13] indicate that the growth rate of the instability mode decreases with increasing streak amplitude. This behavior is shown in Fig. 20 where σ_r is plotted versus k_x of the instability mode in the absence of streaks and when $B=14\%$. The symbols are obtained from our numerical solution and the lines are from Cossu and Brandt.[13] The value of the maximum growth rate of the instability was also recorded over a range of streak amplitudes, and is reported in Table I. The influence of steady streaks is the consistent reduction in the growth rate of the instability, and good quantitative agreement is demonstrated between our solution and the literature.

Resolution tests were carried out in order to ensure convergence of the Floquet expansion in both periodic directions. The resolution requirements in the streamwise direction were consistent with Herbert.[7] The resolution test for the spanwise Floquet expansion showed higher sensitivity to the truncation. The recommended resolution is $N=50$ Chebyshev polynomials for the discretization and $N_B=5$ spanwise Floquet modes in the expansion.

[1] X. Wu and M. Choudhari, "Linear and nonlinear instabilities of a Blasius boundary layer perturbed by streamwise vortices. Part 2. Intermittent instability induced by long-wavelength Klebanoff modes," J. Fluid Mech. **483**, 249 (2003).
[2] A. V. Boiko, K. J. A. Westin, B. G. B. Klingmann, V. V. Kozlov, and P. H. Alfredsson, "Experiments in a boundary layer subjected to freestream turbulence. Part II. The role of TS-waves in the transition process," J. Fluid Mech. **281**, 219 (1994).
[3] C. Cossu and L. Brandt, "Stabilization of Tollmien–Schlichting waves by finite amplitude optimal streaks in the Blasius boundary layer," Phys. Fluids **14**, L57 (2002).
[4] H. F. Fasel, "Numerical investigation of the interaction of the Klebanoff-mode with a Tollmien–Schlichting," J. Fluid Mech. **450**, 1 (2002).
[5] Y. Liu, "Transition to turbulence by mode interaction," Ph.D. thesis, Stanford University, 2007.
[6] Y. Liu, T. A. Zaki, and P. A. Durbin, "Boundary layer transition by interaction of discrete and continuous modes," J. Fluid Mech. **604**, 199 (2007).
[7] T. Herbert, "Secondary instability of boundary layers," Annu. Rev. Fluid Mech. **20**, 487 (1988).
[8] J. Fransson, L. Brandt, A. Talamelli, and C. Cossu, "Experimental study of the stabilization of Tollmien–Schlichting waves by finite amplitude streaks," Phys. Fluids **17**, 054110 (2005).
[9] P. S. Klebanoff, "Effect of freestream turbulence on the laminar boundary layer," Bull. Am. Phys. Soc. **10**, 1323 (1971).
[10] O. M. Phillips, "Shear-flow turbulence," Annu. Rev. Fluid Mech. **1**, 245 (1969).
[11] T. A. Zaki and P. A. Durbin, "Mode interaction and the bypass route to transition," J. Fluid Mech. **531**, 85 (2005).
[12] T. A. Zaki and P. A. Durbin, "Continuous mode transition and the effects of pressure gradient," J. Fluid Mech. **563**, 357 (2006).
[13] C. Cossu and L. Brandt, "On Tollmien–Schlichting like waves in streaky boundary layers," Eur. J. Mech. B/Fluids **23**, 815 (2004).
[14] A. D. D. Craik, "Nonlinear resonant instability in boundary layers," J. Fluid Mech. **50**, 393 (1971).
[15] T. Herbert, "Secondary instability of plane channel flow to subharmonic three-dimensional disturbances," Phys. Fluids **26**, 871 (1983).
[16] M. E. Goldstein and D. W. Wundrow, "Interaction of oblique instability waves with weak streamwise vortices," J. Fluid Mech. **284**, 377 (1995).
[17] F. Li and M. R. Malik, "Fundamental and subharmonic secondary instabilities of Görtler vortices," J. Fluid Mech. **297**, 77 (1995).